ELSEVIER

Solid State Sciences 4 (2002) 507–513

Solid State Sciences

www.elsevier.com/locate/ssscie

Mössbauer spectral evidence for next-nearest neighbor interactions within the alluaudite structure of $Na_{1-x}Li_xMnFe_2(PO_4)_3$

Raphaël P. Hermann [a], Frédéric Hatert [b], André-Mathieu Fransolet [b], Gary J. Long [c], Fernande Grandjean [a,*]

[a] *Institut de Physique, B5, Université de Liège, B-4000 Sart-Tilman, Belgium*

[b] *Laboratoire de Minéralogie, B18, Université de Liège, B-4000 Sart-Tilman, Belgium*

[c] *Department of Chemistry, University of Missouri-Rolla, Rolla, MO 65409-0010, USA*

Received 8 October 2001; received in revised form 26 November 2001; accepted 11 December 2001

Abstract

The Mössbauer spectra of the $Na_{1-x}Li_xMnFe_2(PO_4)_3$ compounds, with $x = 0.00$, 0.25, 0.50, and 0.75, have been measured between 90 and 295 K and analyzed in terms of a model which takes into account the next-nearest neighbor interactions within the alluaudite structure. Surprisingly, the spectra reveal an unexpected presence of iron(II) in these compounds; the amount of iron(II) is observed to decrease from 19 to 15 atomic percent of the total iron content with increasing x. The temperature dependence of the Fe^{2+} and Fe^{3+} isomer shifts agrees with that expected from a second-order Doppler shift and the resulting iron vibrating masses and Mössbauer lattice temperatures are within the expected range of values for iron cations in an octahedral environment. The temperature dependence of the Fe^{2+} quadrupole splitting has been fit with the Ingalls' model and the results yield a ground state orbital splitting of ca. 500 cm^{-1} for the iron(II) sites. The compositional dependence of the isomer shifts and Fe^{2+} content can be understood in terms of a decrease in the unit-cell volume with increasing substitution of sodium by lithium, a substitution which does not influence the observed quadrupole splittings.

1. Introduction

The generic term alluaudite designates a group of sodium, manganese, and iron-bearing phosphate minerals which are found in granitic pegmatites. These minerals have a chemical composition ranging between $Na_2MnFe_2(PO_4)_3$, which contains equal amounts of Fe^{2+} and Fe^{3+}, and $NaMnFe_2(PO_4)_3$, which contains only Fe^{3+}.

The alluaudite crystal structure was first described by Moore [1] who studied a natural sample from the Buranga pegmatite in Rwanda. This author proposed X(2)X(1)M(1)-M(2)$_2$[PO$_4$]$_3$ as the general formula of alluaudite. Its monoclinic structure with the C2/c space group consists of kinked chains of edge-sharing octahedra stacked parallel to {1 0 1}. These chains are formed by a succession of M(2) octahedral pairs linked by highly distorted M(1) octahedra. Equivalent chains are connected together in the *b* direction by the P(1) and P(2) phosphate tetrahedra to form sheets oriented perpendicular to [0 1 0]. These interconnected sheets produce channels parallel to the *c* axis, channels which contain the distorted cubic X(1) site and the four-coordinated X(2) site.

During the past decade, the increasing number of structural studies performed on synthetic compounds exhibiting the alluaudite structure clearly demonstrate the existence of three cationic sites not reported earlier [1]. These sites are located in the channels on crystallographic positions which are different from those of X(1) and X(2) noted above. Based on detailed structural studies, Hatert et al. [2] proposed a new general formula, [A(2)A(2)′][A(1)A(1)′A(1)″$_2$]M(1)M(2)$_2$-[PO$_4$]$_3$, for alluaudite-type compounds. These authors pointed out that, in contrast to the M sites, the A crystallographic sites of the alluaudite structure can be partially or totally empty. The majority of alluaudites studied to date contain atoms on the A(1) and A(2)′ sites and have vacancies on the A(2), A(1)′, and A(1)″ sites.

Because iron phosphates have numerous practical applications [3], such as corrosion inhibition, passivation of metal surfaces, and catalysis, many synthetic iron phosphates have been synthesized and shown to crystallize in the alluaudite-

* Correspondence and reprints.
E-mail addresses: r.hermann@ulg.ac.be (R.P. Hermann), fhatert@ulg.ac.be (F. Hatert), amfransolet@ulg.ac.be (A.-M. Fransolet), glong@umr.edu (G.J. Long), fgrandjean@ulg.ac.be (F. Grandjean).

1293-2558/02/$ – see front matter
PII: S1293-2558(02)01278-5

Table 1
Unit-cell volume, average Fe–O bond distance, and Fe^{2+} content in $Na_{1-x}Li_xMnFe_2(PO_4)_3$

x	V (Å^3)	Fe–O (Å)	Fe^{2+} (%)[a]
0.00	877.3(2)	2.046(1)	11.8
0.25	873.0(2)	–	11.5
0.50	868.6(3)	2.038(2)	12.0
0.75	865.5(3)	–	10.6

[a] Atomic percent of the total iron content obtained from wet chemical analysis.

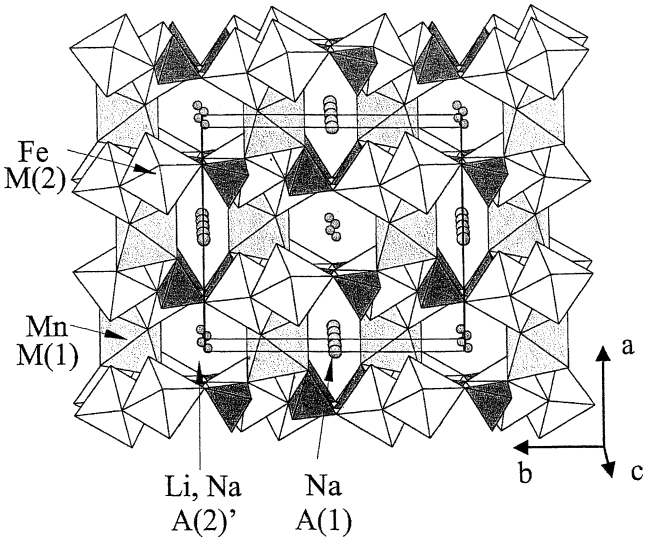

Fig. 1. The crystal structure of $Na_{1-x}Li_xMnFe_2(PO_4)_3$.

like structure. The possibility of inserting variable amounts of lithium into the channels of the alluaudite structure makes the title compounds of value as potential battery materials [4]. The present Mössbauer spectral study is part of our investigation [3,5–7] of the iron electronic and magnetic properties in the sodium, manganese, and iron-bearing alluaudites and related compounds, a study which was initiated with the goal of investigating the influence of small lithium ions located on the large cationic sites.

In order to better understand the crystal chemistry of lithium in the alluaudite structure, Hatert et al. [2] investigated the $Na_{1-x}Li_xMnFe_2(PO_4)_3$ solid solutions. Lithium was inserted into these compounds up to $x = 0.9$ and the unit-cell volume was found to decrease with increasing lithium content, see Table 1. A single-crystal structure refinement of the alluaudite-like compound $Na_{0.5}Li_{0.5}MnFe_2(PO_4)_3$ has also been reported by Hatert et al. [2], and the resulting structure is shown in Fig. 1. The refinement indicates that lithium occupies the $(4 + 4)$-coordinated A(2)′ site, a site which exhibits a morphology corresponding to the gable disphenoid described by Moore [8] in the homeotypic wyllieite structure. A comparison [2] with the cationic distribution in $NaMnFe_2(PO_4)_3$ suggests a replacement of a vacancy with a lithium ion on the A(2)′ site, and of sodium ion with a vacancy on the A(1) site. Consequently, the substitution mechanism, $V + Na^+ \rightarrow Li^+ + V$, where V denotes a lattice vacancy, was proposed [2] for the insertion of lithium into the $Na_{1-x}Li_xMnFe_2(PO_4)_3$ solid solutions. On the basis of a steric argument Hatert et al. [2] also proposed that the M(1) site is occupied by manganese, and that the M(2) site is occupied by iron. A similar occupation of the M(1) site by manganese and the M(2) sites by manganese and iron has been deduced from a neutron diffraction study [9] of the alluaudite compound, $Ag_2FeMn_2(PO_4)_3$. Wet chemical analyses have indicated that significant amounts of Fe^{2+}, see Table 1, are present in the compounds and an earlier discussion [2] of the M(2) site bond distances indicates that Fe^{2+} probably shares the M(2) site with Fe^{3+}. The Mössbauer spectral study was initiated in order to investigate the iron site occupation, the iron oxidation state, and the influence, if any, of the substitution of Li^+ for Na^+ upon the iron hyperfine parameters.

2. Experimental

$Na_{1-x}Li_xMnFe_2(PO_4)_3$ solid solutions, with $x = 0.00$, 0.25, 0.50, and 0.75, have been synthesized through a solid state reaction carried out in air. Stoichiometric quantities of $NaHCO_3$, Li_2CO_3, MnO, $FeSO_4{\cdot}7H_2O$, and $(NH_4)H_2PO_4$ were dissolved in concentrated nitric acid and the resulting solution was evaporated to dryness. The dry residue was progressively heated in a platinum crucible, at a heating rate of $500\,^\circ C\,h^{-1}$, to the congruent fusion temperature of 950 °C and then maintained at this temperature for 15 to 20 hours. Alluaudite crystals were obtained by quenching the product in air. Wet chemical analyses, unit-cell parameters, and crystal structure refinement data for the title compounds have been reported by Hatert et al. [2].

The Mössbauer spectra were measured between 90 and 295 K on a constant-acceleration spectrometer which utilized a room temperature rhodium matrix cobalt-57 source and was calibrated at room temperature with α-iron foil. The Mössbauer spectral absorbers contained 26, 34, 23, and 14 $mg\,cm^{-2}$ of powder for $x = 0.00$, 0.25, 0.50, and 0.75, respectively. The absorber thickness was chosen as a compromise between the ideal thickness [10], which yields the ideal signal to noise ratio, and the thin absorber limit. This compromise permits a temperature dependent study with the same absorber within reasonable counting times.

3. Mössbauer spectral results

3.1. Analysis of the spectra

The 90 K Mössbauer spectra of $Na_{1-x}Li_xMnFe_2(PO_4)_3$, with $x = 0.00$, 0.25, 0.50, and 0.75, are shown in Fig. 2 and the spectra of $Na_{0.5}Li_{0.5}MnFe_2(PO_4)_3$, obtained at five different temperatures, are shown in Fig. 3.

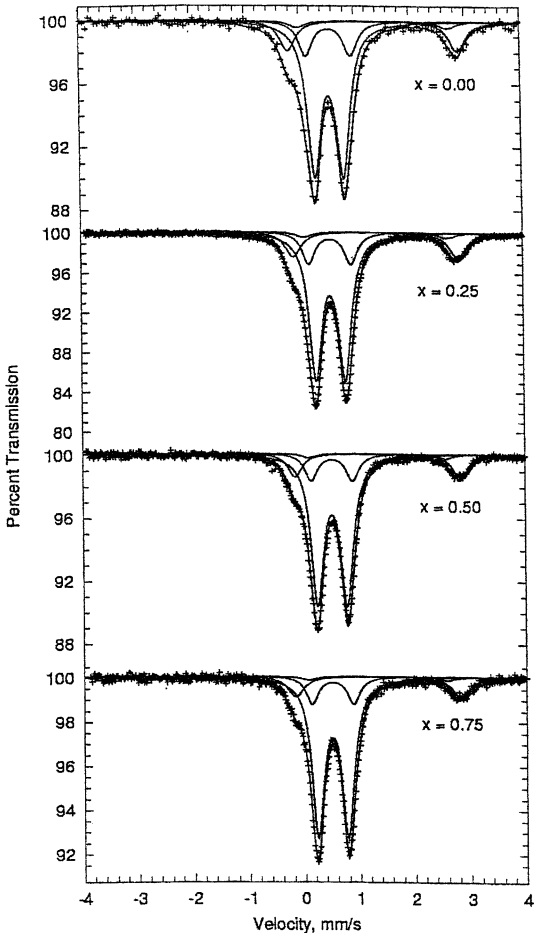

Fig. 2. The Mössbauer spectra of $Na_{1-x}Li_xMnFe_2(PO_4)_3$ obtained at 90 K.

The observation of two absorption bands at ca. 0.5 and 2.8 mm s^{-1} in these spectra suggests that they should be fit with at least two doublets, the first, with a small isomer shift and quadrupole splitting, assigned to Fe^{3+} and the second, with a large isomer shift and quadrupole splitting, assigned to Fe^{2+}. Furthermore, the poor fits obtained with this simplistic model yield broad linewidths of ca. 0.45 mm s^{-1} and suggest that a reasonable fit of these spectra will require at least two Fe^{3+} doublets and two Fe^{2+} doublets.

A model for the analysis of the Mössbauer spectra has been developed on the basis of the alluaudite crystal structure [2]. If g is the Fe^{2+} and $1-g$ is the Fe^{3+} fractional occupancy of the M(2) site, four different configurations of the octahedra, as shown in Fig. 4, are possible; their corresponding probabilities are also given in Fig. 4. The Mössbauer spectrum would then be expected to exhibit two Fe^{2+} and two Fe^{3+} quadrupole doublets corresponding to these four configurations. If the recoil free fractions for Fe^{2+} and Fe^{3+} are assumed to be equal [11], an assumption which is valid at low temperature, i.e., below 100 K, the areas of these doublets are proportional to the probabilities of the four configurations. A fit with these hypotheses requires 15 adjustable parameters. However, preliminary fits have indicated that both the isomer shifts of the two Fe^{2+} and

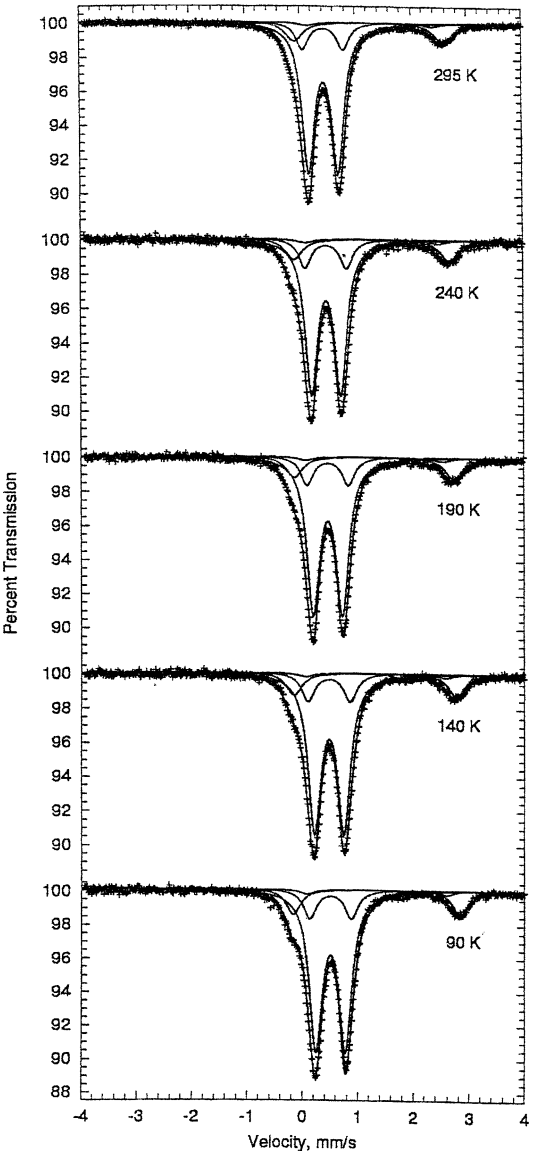

Fig. 3. The Mössbauer spectra of $Na_{0.5}Li_{0.5}MnFe_2(PO_4)_3$ obtained at the indicated temperatures.

the isomer shifts of the two Fe^{3+} doublets were identical within the experimental error of ± 0.002 mm s^{-1}. Thus, to both reduce the number of parameters and use a maximum of constraints to fit the spectra, we have used the same isomer shift and linewidths for both the Fe^{2+} and Fe^{3+} doublets. Including the baseline and total absorption area, this model has 11 adjustable parameters, the Fe^{2+} fraction, g, the isomer shifts, δ, for Fe^{2+} and Fe^{3+}, the linewidths, Γ, for Fe^{2+} and Fe^{3+}, and the quadrupole splittings, ΔE_Q, corresponding to the four configurations listed in Fig. 4.

The fitted values of the Mössbauer spectral parameters are given in Table 2. The fraction, g, of Fe^{2+} obtained from Mössbauer spectroscopy and ranging from 15.1 to 19.1 atomic percent at 90 K, is substantially larger than that obtained by wet chemical analysis which gives values ranging from 10.6 to 12 percent. As is well-known [11],

Table 2
Mössbauer spectral parameters for $Na_{1-x}Li_xMnFe_2(PO_4)_3$

				Fe^{3+} (mm s^{-1})				Fe^{2+} (mm s^{-1})			
x	T (K)	Area[a]	g (%)	δ[b]	$\Delta E_{Q,3-3}$	$\Delta E_{Q,3-2}$	Γ	δ[b]	$\Delta E_{Q,2-3}$	$\Delta E_{Q,2-2}$	Γ
0.00	295	0.231(1)	17.8(4)	0.428(1)	0.520(1)	0.77(1)	0.309(2)	1.253(5)	2.71(1)	2.09(7)	0.43(1)
	240	0.237(1)	18.2(4)	0.444(1)	0.521(1)	0.77(1)	0.298(2)	1.264(4)	2.78(1)	2.19(7)	0.42(1)
	190	0.247(1)	18.3(4)	0.470(1)	0.522(2)	0.77(1)	0.309(2)	1.301(5)	2.87(1)	2.32(7)	0.42(2)
	140	0.255(1)	19.3(4)	0.493(1)	0.524(2)	0.77(1)	0.301(2)	1.325(4)	2.96(1)	2.44(6)	0.41(1)
	90	0.262(1)	19.1(4)	0.513(1)	0.525(1)	0.77(1)	0.294(2)	1.341(4)	3.04(1)	2.48(5)	0.38(1)
0.25	295	0.229(1)	16.8(3)	0.419(1)	0.529(1)	0.75(1)	0.294(2)	1.222(4)	2.62(1)	2.04(5)	0.41(1)
	240	0.251(1)	18.0(3)	0.456(1)	0.528(1)	0.76(1)	0.287(2)	1.272(3)	2.76(1)	2.36(5)	0.40(1)
	190	0.261(1)	18.2(3)	0.478(1)	0.526(1)	0.77(1)	0.290(2)	1.298(3)	2.84(1)	2.46(5)	0.39(1)
	140	0.270(1)	18.0(3)	0.497(1)	0.530(1)	0.77(1)	0.287(2)	1.316(3)	2.92(1)	2.56(5)	0.38(1)
	90	0.283(1)	18.5(3)	0.515(1)	0.530(1)	0.77(1)	0.289(2)	1.334(3)	2.98(1)	2.59(4)	0.37(1)
0.50	295	0.223(1)	15.9(3)	0.422(1)	0.533(1)	0.73(1)	0.276(2)	1.241(4)	2.67(1)	2.25(6)	0.39(1)
	240	0.230(1)	16.3(5)	0.449(1)	0.530(2)	0.75(1)	0.272(2)	1.263(5)	2.78(1)	2.39(8)	0.38(2)
	190	0.237(1)	15.9(4)	0.467(5)	0.530(2)	0.75(1)	0.278(2)	1.288(4)	2.85(1)	2.45(7)	0.37(2)
	140	0.242(1)	15.7(4)	0.485(1)	0.535(2)	0.76(1)	0.283(2)	1.306(5)	2.91(1)	2.51(7)	0.36(2)
	90	0.244(1)	16.2(4)	0.511(1)	0.536(2)	0.76(1)	0.275(3)	1.335(5)	2.98(1)	2.50(6)	0.32(1)
0.75	295	0.246(1)	14.6(5)	0.413(1)	0.540(2)	0.73(1)	0.272(3)	1.231(6)	2.64(1)	2.17(9)	0.39(2)
	240	0.264(1)	14.2(5)	0.443(1)	0.540(2)	0.75(1)	0.272(2)	1.253(6)	2.76(1)	2.35(9)	0.38(2)
	190	0.275(1)	14.9(5)	0.465(1)	0.538(2)	0.75(1)	0.270(2)	1.278(5)	2.84(1)	2.46(9)	0.37(2)
	140	0.285(2)	14.7(5)	0.485(1)	0.543(2)	0.75(1)	0.272(2)	1.307(6)	2.91(1)	2.53(9)	0.39(2)
	90	0.296(2)	15.1(5)	0.501(1)	0.546(2)	0.75(1)	0.274(3)	1.316(6)	2.99(1)	2.52(9)	0.36(2)

[a] The total absorption area has units of $[(\%\,\varepsilon)(\text{mm s}^{-1})]\,\text{mg}^{-1}$. [b] Relative to α-iron at 295 K.

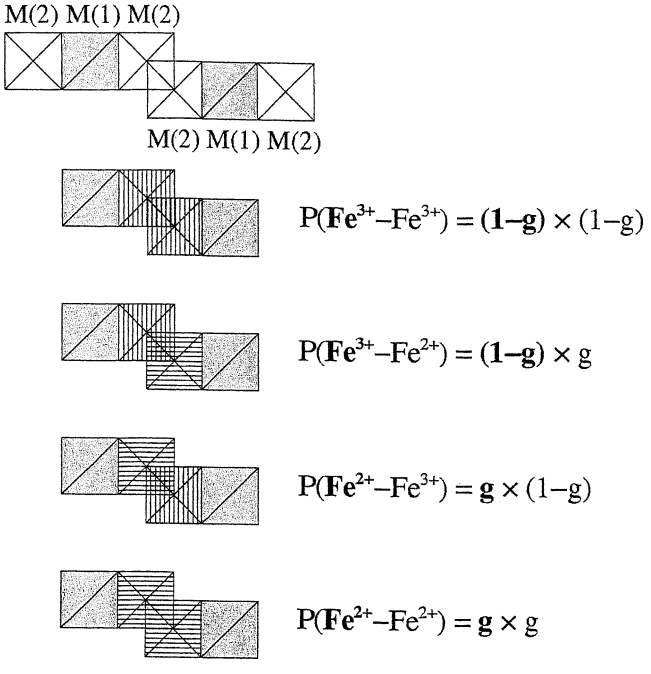

Fig. 4. The four different configurations of next-nearest neighbor M(2) sites occupied by Fe^{3+} and Fe^{2+} and the probabilities as obtained for the ion in bold face type. The vertical lines represent Fe^{3+} and the horizontal lines Fe^{2+}.

the Fe^{2+} recoil-free fraction decreases faster with increasing temperature than does that of Fe^{3+}, a difference which explains the slight decrease in g observed with increasing temperature. The following discussion will use the values of g obtained at 90 K.

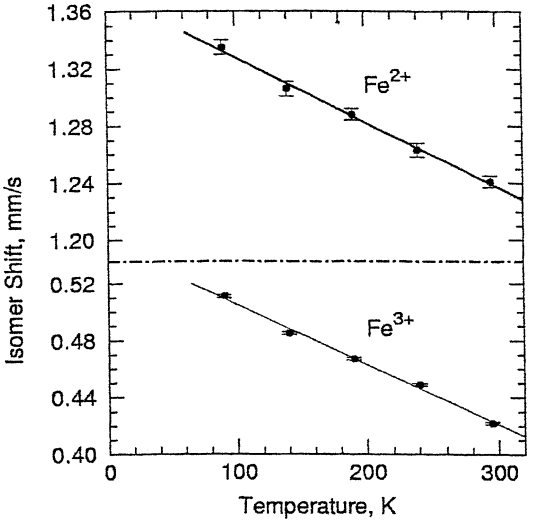

Fig. 5. The temperature dependence of the isomer shifts in $Na_{0.5}Li_{0.5}MnFe_2(PO_4)_3$.

3.2. Temperature dependence

In agreement with the second order Doppler shift, both the Fe^{2+} and Fe^{3+} isomer shifts decrease with increasing temperature, as is illustrated in Fig. 5 for $Na_{0.5}Li_{0.5}MnFe_2(PO_4)_3$. A similar behavior has been observed for the other compounds understudy herein. These decreases have been fit with straight lines and the slopes, $d\delta/dT$, are given in Table 3. From these slopes and that of the logarithm of the absorption area, $d(\ln \text{Area})/dT$, the effective vibrating masses and Mössbauer lattice temperatures, θ_M, have been calcu-

Table 3
Parameters obtained from the temperature dependence of the Mössbauer spectra

x	0.00	0.25	0.50	0.75
$10^4 \times d\delta/dT$ Fe^{2+} ($mm\,s^{-1}\,K^{-1}$)	−4.6(2)	−5.3(6)	−4.5(2)	−4.5(4)
$10^4 \times d\delta/dT$ Fe^{3+} ($mm\,s^{-1}\,K^{-1}$)	−4.3(5)	−4.6(3)	−4.2(2)	−4.4(3)
$10^4 \times d(\ln \text{Area})/dT$ (K^{-1})	−6.4(4)	−10(1)	−4.7(5)	−8.9(8)
M_{eff} Fe^{2+} ($g\,mol^{-1}$)	90(9)	79(10)	92(4)	93(7)
M_{eff} Fe^{3+} ($g\,mol^{-1}$)	96(4)	91(7)	99(4)	95(7)
θ'_M Fe^{2+} (K)	369(21)	316(26)	423(23)	307(18)
θ'_M Fe^{3+} (K)	357(13)	295(20)	407(23)	302(17)
Δ_{2-3} (cm^{-1})	542(30)	500(30)	522(30)	503(30)
$\Delta E_{Q,2-3}(0)$ ($mm\,s^{-1}$)	3.05[a]	3.05[a]	3.00[a]	3.00[a]
Δ_{2-2} (cm^{-1})	495(20)	460(30)	601(10)	523(20)
$\Delta E_{Q,2-2}(0)$ ($mm\,s^{-1}$)	2.46(2)	2.61(4)	2.507(8)	2.54(2)

[a] Parameter constrained to the value given.

lated [12] and are also given in Table 3. The Mössbauer lattice temperatures are between 300 and 425 K, hence the linear approximation used for the temperature dependence of the isomer shift between 90 and 295 K is a rather rough approximation [13] and the relatively large effective vibrating masses of ca. 90 $g\,mol^{-1}$ are probably overestimated because the investigated temperature range is too small. However, the reasonable temperature dependence of the isomer shifts serves to validate the fitting model. The Mössbauer lattice temperatures between 300 and 425 K fall within the range of 288 to 460 K observed for iron atoms in the octahedral sites of the spinel structure [14]. The Fe^{2+} Mössbauer lattice temperatures are systematically larger than the Fe^{3+} Mössbauer lattice temperatures probably because the larger Fe^{2+} cation is more tightly bound in the M(2) site, a site normally occupied by the smaller Fe^{3+} cation. A more detailed discussion of the temperature dependence of the isomer shift would require a study at temperatures above room temperature.

As expected for high-spin Fe^{3+}, the quadrupole splittings, $\Delta E_{Q,3-3}$ and $\Delta E_{Q,3-2}$, are temperature independent within experimental error. In contrast and as expected, the Fe^{2+} quadrupole splittings, $\Delta E_{Q,2-2}$ and $\Delta E_{Q,2-3}$, decrease substantially with increasing temperature, as is shown in Fig. 6. In the Ingalls' model [15] the temperature dependence of the Fe^{2+} quadrupole splitting, ΔE_Q, in a distorted environment may be calculated from the expression,

$$\Delta E_Q = \Delta E_Q(0) \times \tanh\left(\frac{\Delta}{2kT}\right),$$

where $\Delta E_Q(0)$ is the quadrupole splitting at 0 K and Δ is the splitting of the iron(II) orbital triplet $^5T_{2g}$ octahedral ground state by low symmetry components of the crystal field. The solid lines shown in Fig. 6 correspond to the best fits of the quadrupole splittings with this model and the parameters, Δ and $\Delta E_Q(0)$ obtained from these fits are given in Table 3. A splitting of ca. 500 cm^{-1} is quite normal for a distorted octahedral environment [16]. The values of $\Delta E_Q(0)$ are poorly determined in the absence

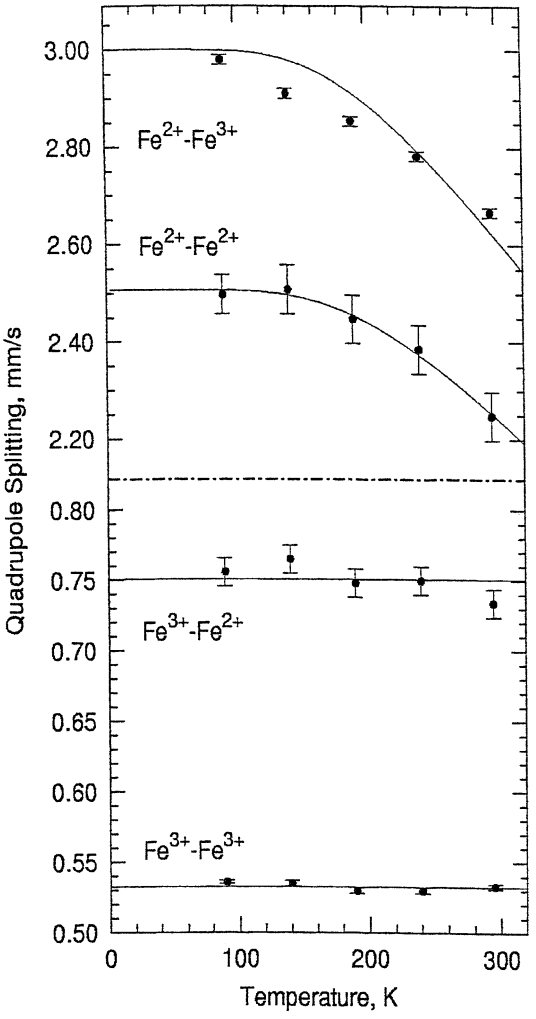

Fig. 6. The temperature dependence of the quadrupole splittings in $Na_{0.5}Li_{0.5}MnFe_2(PO_4)_3$. The solid lines represent the fit with Ingalls's [15] model.

of measurements below 85 K, measurements which would not be very helpful, as in the magnetically ordered phase, the very weak Fe^{2+} sextets will be obscured by the Fe^{3+} sextets. However, the values given in Table 3 are quite normal for Fe^{2+} ions and agree with those observed [5,7] in other alluaudite compounds. The failure of the Ingalls' model to more adequately fit the Fe^{2+}–Fe^{3+} quadrupole splittings, see Fig. 6, is an indication that Δ is changing with temperature, a change which is not considered within this model. Further, the virtually linear temperature dependence of the Fe^{2+}–Fe^{3+} quadrupole splitting, with a slope of ca. -15×10^{-4} $mm\,s^{-1}\,K^{-1}$, see Fig. 6, is reminiscent of the linear temperature dependence with a slope of ca. -17×10^{-4} $mm\,s^{-1}\,K^{-1}$, observed [17] for the Fe^{2+} ion in a trigonal coordination environment in the $(Fe,Zn)_2Mo_3O_8$ compounds. Unfortunately, a fit of the five experimental values of the quadrupole splittings, see Fig. 6, with a model [17] which uses four parameters, is not realistic. We believe that the temperature dependence of the Fe^{2+}–Fe^{3+} quadrupole splitting is a consequence of the varying thermal

population of the low lying crystal field states of the highly distorted M(2) site of the alluaudite structure [2].

3.3. Compositional dependence

The correlation between the unit-cell volume and the Fe^{2+} content obtained from the Mössbauer spectral analysis is shown in Fig. 7. The decrease in the Fe^{2+} content with increasing x can be qualitatively understood in terms of a decrease with x of the unit-cell volume, see Table 1, and the concomitant decrease of the M(2) site volume. Indeed, as the M(2) site volume decreases, it can accommodate fewer of the larger Fe^{2+} ions.

The isomer shift values given in Table 2 indicate that there is a slight decrease in the isomer shift with increasing x, a decrease which is consistent with the concomitant decrease in unit-cell volume and the consequent decrease in the Fe–O bond distance, see Table 1. Not too surprisingly, there is no significant compositional dependence of the quadrupole splittings because the substitution of Na^+ by Li^+ takes place at a site which is rather remote from the iron ions.

4. Discussion and conclusion

The iron-57 Mössbauer spectra of $Na_{1-x}Li_xMnFe_2(PO_4)_3$, with $x = 0.00$, 0.25, 0.50, and 0.75, have been analyzed with a model which takes into account the influence on the hyperfine parameters of the next-nearest neighbors of the iron M(2) site. A similar next-nearest neighbor effect has already been observed [18] in phosphate minerals in which the distribution of manganese and iron ions in the next-nearest neighbor environment of an iron ion gives rise to changes in quadrupole splittings, changes which are quite similar to those observed herein. The model used herein to fit the intricate Mössbauer spectra may not be unique. However, the consistent temperature and compositional dependencies of the hyperfine parameters, see Figs. 5–7, serve to validate this model. Further, a similar analysis [6] of the Mössbauer spectra of the $NaMnFe_{2-2x}In_{2x}(PO_4)_3$ compounds with the alluaudite structure is equally successful and confirms the validity of the model.

A large number of synthetic iron phosphates, Fe_2PO_5 [19], Fe_9PO_{12} [20], $NaFe_{3.67}(PO_4)_3$ [3] and $SrFe_3(PO_4)_3$ [5], and phosphate minerals, $Li(Fe_{1-x}Mn_x)PO_4$, triphylite [18], $Li_x(Fe_{1-x}Mn_x)PO_4$, ferrisicklerite [18], $(Fe_{1-x}Mn_x)$-PO_4, heterosite [18], $NaMnFeAl(PO_4)_3$, rosemaryite [21], $Fe_3(PO_4)_2(OH)_2$, barbosalite [22], and $Cu_{3-x}Fe_{4+x}(PO_4)_6$ [23] have been investigated by iron-57 Mössbauer spectroscopy. In all of these phosphates, the iron cations are in a distorted octahedral environment. The correlation between the quadrupole splitting and the isomer shift observed in these compounds and those studied herein at 295 K is shown in Fig. 8. Two regions, corresponding to the Fe^{2+} and Fe^{3+} cations, clearly appear in Fig. 8. In both regions the closed symbols, corresponding to the phosphates crystallizing with the alluaudite structure, are closely grouped together. Thus we can conclude that at 295 K the Fe^{3+} ions in the alluaudite structure are characterized by isomer shifts between 0.41 and 0.47 mm s^{-1} and by quadrupole splittings between 0.5 and 0.9 mm s^{-1}, whereas the Fe^{2+} ions are characterized by isomer shifts between 1.1 and 1.3 mm s^{-1} and quadrupole splittings between 2.0 and 2.8 mm s^{-1}. A more detailed discussion of the relationship between the isomer shifts obtained for different iron phosphates and their Fe–O mean

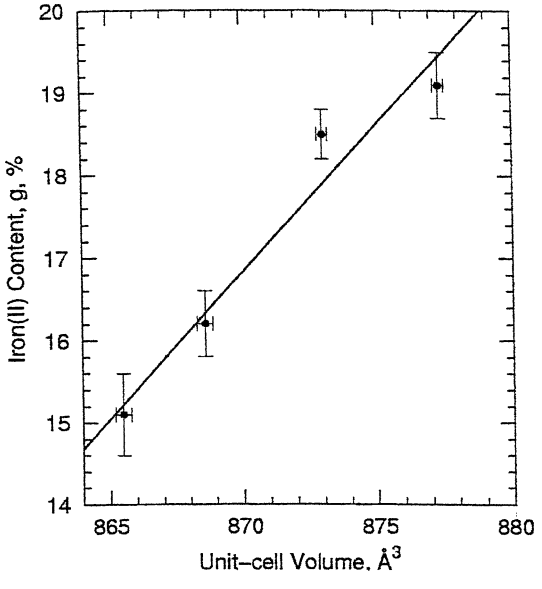

Fig. 7. The correlation between the Fe^{2+} content, obtained from Mössbauer spectral fits, and the unit-cell volume of $Na_{1-x}Li_xMnFe_2(PO_4)_3$.

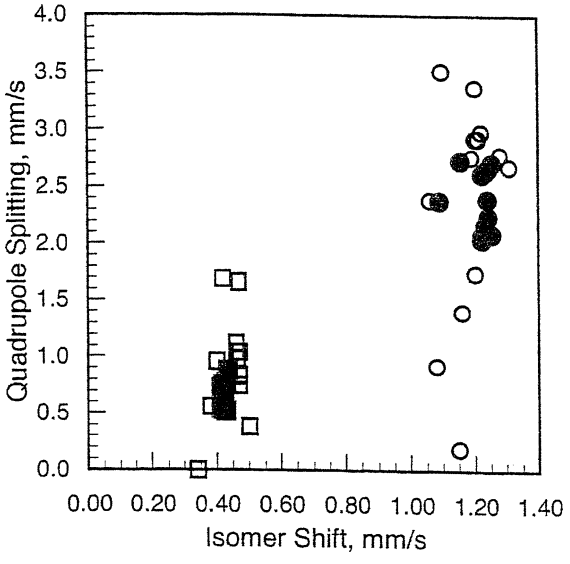

Fig. 8. The correlation between the quadrupole splitting and the isomer shift in various iron phosphates. The closed symbols represent phosphates with the alluaudite structure and the open symbols represent phosphates with other structures. The squares and circles represent the Fe^{3+} and Fe^{2+} cations, respectively. Data were obtained from Refs. [2,4,18–24].

bond distances will be presented in a subsequent paper [6] on $NaMnFe_{2-2x}In_{2x}(PO_4)_3$, solid solutions which also have the alluaudite structure.

This Mössbauer spectral study of $Na_{1-x}Li_xMnFe_2(PO_4)_3$ indicates that the substitution of a sodium ion by a lithium ion does not influence the quadrupole splittings of the iron M(2) site because the steric effect of this substitution occurs at a site remote from the iron ions. In contrast, this substitution decreases the Fe^{2+} content and the isomer shifts in $Na_{1-x}Li_xMnFe_2(PO_4)_3$, with a concomitant decrease of the unit-cell volume.

Acknowledgements

The authors acknowledge the financial support of the Fonds National de la Recherche Scientifique, Belgium, for grant 9.4565.95 and for a visiting professorship for G.J.L. during the 2000–2001 academic year.

References

[1] P.B. Moore, Am. Mineral. 56 (1971) 1955.
[2] F. Hatert, P. Keller, F. Lissner, D. Antenucci, A.-M. Fransolet, Eur. J. Mineral. 12 (2000) 847.
[3] M.B. Korzenski, G.L. Schimek, J.W. Kolis, G.J. Long, J. Solid State Chem. 139 (1998) 152.
[4] A.S. Andersson, Ph.D. Thesis, Uppsala University, 2000;
A.B. Bykov, A.P. Chirkin, L.N. Demyanets, Solid State Ionics 38 (1990) 31;
A.K. Ivanov-Schitz, J. Schoonman, Solid State Ionics 91 (1996) 93;
C. Masquelier, A.K. Padhi, K.S. Nanjundaswamy, J.B. Goodenough, J. Solid State Chem. 135 (1998) 228.
[5] M.B. Korzenski, J.W. Kolis, G.J. Long, J. Solid State Chem. 147 (1999) 390.
[6] F. Hatert, R.P. Hermann, A.-M. Fransolet, G.J. Long, F. Grandjean, Am. Mineral., submitted for publication.
[7] G.J. Long, F. Hatert, A.-M. Fransolet, J. Delwiche, M.J. Hubin-Franskin, F. Grandjean, Phys. Chem. Miner., in preparation.
[8] P.B. Moore, Bull. Minéral. 104 (1981) 536.
[9] N. Chouaibi, A. Daidouh, C. Pico, A. Santrich, M.L. Veiga, J. Solid State Chem. 159 (2001) 46.
[10] G.J. Long, T.E. Cranshaw, G. Longworth, Mössbauer Effect Reference and Data Journal 6 (1983) 42.
[11] E. De Grave, A. Van Alboom, Phys. Chem. Miner. 18 (1991) 337.
[12] R.H. Herber, in: R.H. Herber (Ed.), Chemical Mössbauer Spectroscopy, Plenum Press, New York, 1984, p. 199.
[13] G.J. Long, D. Hautot, F. Grandjean, G.P. Meisner, D.T. Morelli, Phys. Rev. B 62 (2000) 6829.
[14] R.E. Vandenberghe, E. De Grave, in: G.J. Long, F. Grandjean (Eds.), Mössbauer Spectroscopy Applied to Inorganic Chemistry, Vol. 3, Plenum Press, New York, 1989, p. 59.
[15] R. Ingalls, Phys. Rev. 133 (1964) A787.
[16] F. Hartmann-Boutron, P. Imbert, J. Appl. Phys. 39 (1968) 775.
[17] F. Varret, H. Czeskleba, F. Hartmann-Boutron, P. Imbert, J. Physique 33 (1972) 549.
[18] Z. Li, I. Shinno, Mineralogical J. 19 (1997) 99.
[19] M. Ijaali, B. Malaman, G. Venturini, C. Gleitzer, G.J. Long, F. Grandjean, J. Phys.: Condens. Matter 3 (1991) 9597.
[20] G.J. Long, C. Gleitzer, Hyperfine Interact. 62 (1990) 147.
[21] R.P. Hermann, F. Hatert, A.-M. Fransolet, F. Grandjean, unpublished results.
[22] G.J. Redhammer, G. Tippelt, G. Roth, W. Lottermoser, G. Amthauer, Phys. Chem. Miner. 27 (2000) 419.
[23] A.A. Belik, A.P. Malakho, K.V. Pokholok, B.I. Lazoryak, S.S. Khasanov, J. Solid State Chem. 150 (2000) 159.
[24] I. Shinno, Z. Li, Am. Mineral. 83 (1998) 1316.